Pushing indium phosphide DHBT frequency to 1.2THz

Researchers claim a record maximum oscillation frequency x breakdown voltage product for any type of transistor.

Switzerland's ETH Zürich claims a record 1.2THz maximum oscillation frequency (f_{MAX}) for a 0.25μmx0.44μm double-heterojunction bipolar transistor (DHBT) [Akshay M. Arabhavi et al, IEEE Transactions on Electron Devices, vol69, issue 4 (April 2022), p2122] (see Figure 1). The materials used were a combination of indium phosphide (InP), gallium indium arsenide (GaInAs) and gallium arsenide antimonide (GaAsSb) with a staggered 'type-II' band alignment. This alleviates electron-blocking effects at the base–collector hetero-junction.

The product of f_{MAX} and open-base common-emitter breakdown voltage (BV_{CEO}) of 6.48THz-V is also claimed to be the highest reported for any type of transistor. Even making the geometric average (square root of product) of f_{MAX} with the 475GHz cut-off (f_T) gives a InP DHBT record product with BV_{CEO}) of over 4THz-V. Gallium nitride high-electron-mobility transistors offer 4.9THz-V with a relaxed definition for breakdown voltage.

According to the team, these achievements result from:

- a tunable base–emitter access distance down to 10nm;
- the use of thicker base contact metals;

(continued overleaf)

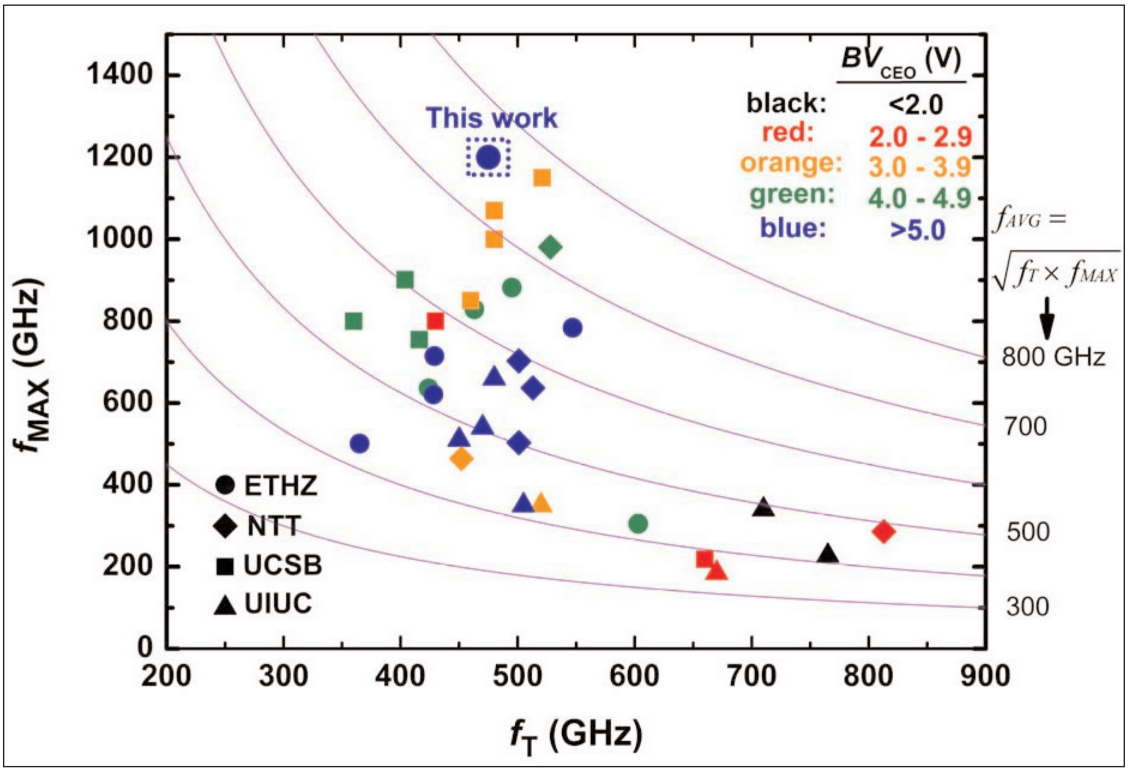

Figure 1. Survey of reported InP DHBT metrics. Breakdown voltages are color-coded.

Figure 2. Semiconductor material structure.

Material	Doping (/cm^3)	Thickness
$Ga_{0.47}In_{0.53}As \rightarrow Ga_{0.25}In_{0.75}As$	Si: 3 9x10^{19}	10nm
InP	Si: 4x10^{19}	20nm
InP	Si: 2.2x10^{16}	5nm
$Ga_{0.22}In_{0.78}P \rightarrow InP$	Si: 2.2x10^{16}	10nm
$Ga_{0.22}In_{0.78}P$	Si: 2.2x10^{16}	5nm
$GaAs_{0.42}Sb_{0.58} \rightarrow GaAs_{0.61}Sb_{0.39}$	C: 8.5x10^{19}	20nm
InP	Si: 1.0x10^{17}	125nm
InP	S: 2 9x10 ^{19}	50nm
$Ga_{0.47}In_{0.53}As$	Si: 4.0x10^{19}	20nm
InP	2 9x10^{19}	300nm
InP semi-insulating substrate		350μm

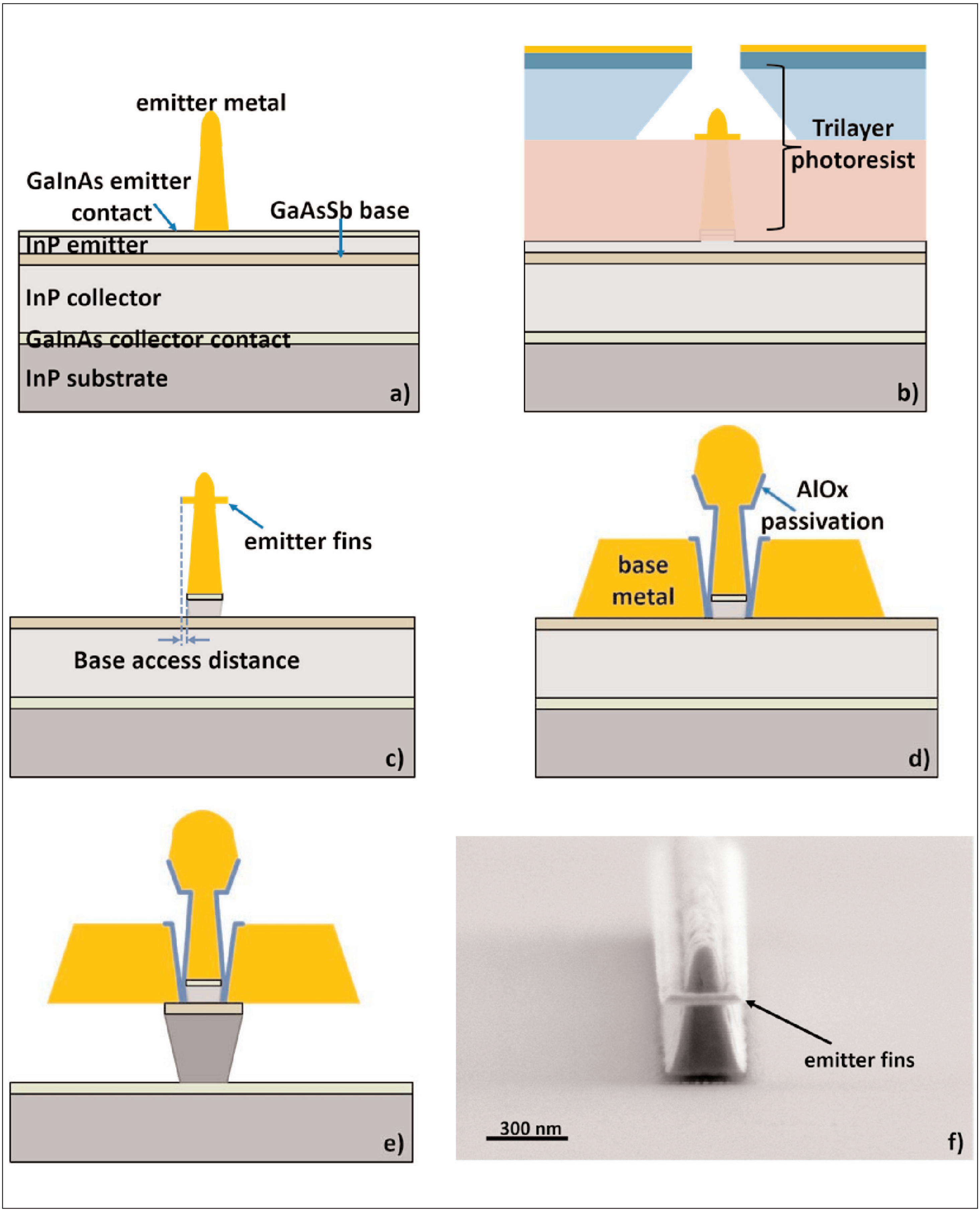

Figure 3. Simplified schematic view of key emitter fin fabrication steps: (a) emitter metal; (b) emitter fin formation using trilayer photoresist; (c) emitter mesa showing the base access distance; (d) self-aligned base contacts and AlO_x passivation; and (e) narrow base–collector mesa. Schematics not to scale. (f) Scanning electron micrograph of emitter after mesa formation.

- minimization of parasitic capacitances and resistances via precise lateral wet etching of the base–collector (B/C) mesa.

The researchers comment: "The present scaling breakthrough, with the availability of THz transistors with larger junction areas capable of operation under high input drive and higher collector voltages, opens opportunities for the generation of significant signal power at mm-wave and sub-mm wave frequencies."

The team sees oscillators and power amplifiers at these high frequencies as being more dependent on high f_{MAX} rather than f_T. The researchers also see the maintenance of high terahertz frequency performance to devices of 1.645μm² area, more than 6x larger than previously reported THz InP DHBTs, as being an important achievement.

The epitaxial semiconductor material (Figure 2) was prepared using metal-organic vapor-phase epitaxy (MOVPE) on 2-inch InP substrate. The gallium indium arsenide emitter layer was graded ($Ga_{0.47}In_{0.53}As \longrightarrow G_{a0.25}In_{0.75}As$) to eliminate the conduction-band offset at the emitter–base (E/B) interface. The gallium arsenide antimonide base layer was also ramped ($GaAs_{0.42}Sb_{0.58} \longrightarrow GaAs_{0.61}Sb_{0.39}$), along with the doping concentration.

Device fabrication began with forming the titanium/platinum/gold emitter electrode (Figure 3). Argon sputtering was used to etch the GaInAs emitter contact layer, while also smoothing the emitter electrode. Horizontal fins were added to the emitter electrode in processes involving a tri-layer photoresist, electron-beam lithography, and electron-beam evaporation and lift-off of the fin metal. The fins set the base access distance in a self-aligning manner.

The emitter mesa was formed by phosphoric acid etch. The base region was then defined with electron-beam lithography, followed by electron-beam evaporation of palladium/nickel/platinum/gold. The fins allow a reduced base access distance to be combined with a thicker base metal layer (~50%) without shorting between the emitter/base contacts, reducing contact resistance. The surfaces of the base and emitter structures were then passivated with atomic layer deposition (ALD) of aluminium oxide (AlO_x).

A sequence of dry and wet etches were used to give an undercut collector mesa with an effective base–collector contact width of 40nm. This distance ensures that "only a transfer length equivalent of base material remains under the base metal contact," the team comments.

The device was planarized using a Teflon-based process and completed with electron-beam evaporated coplanar probe pads.

The open-base common-emitter breakdown voltage BV_{CEO} was 5.4V at a collector current density of 1kA/cm². Single-pole extrapolations from Mason's unilateral power gain and common-emitter short-circuit current-gain small-signal radio frequency (RF) measurements up to 50GHz gave peak maximum oscillation (f_{MAX}) and cut-off (f_T) frequencies of 1.2THz and 475GHz, respectively, with 1V collector–emitter bias (V_{CE}).

A single-finger (0.175μmx9.4μm) DHBT biased for class-A operation was subjected to active-loop load-pull continuous wave (cw) large-signal measurements at 94GHz. The power-added efficiency (PAE) was 32.5% (40% collector efficiency) with 1.6V V_{CE} bias and 1mA base current (I_B). The saturated output power ($P_{out,sat}$) was 8.73dBm and the gain 7.8dB.

Increasing V_{CE} to 1.9V enabled a higher peak $P_{out,sat}$ at the expense of lower PAE: 10.4dBm (832mV V_{BE}) and 29.3%, respectively. The $P_{out,sat}$ density was 6.67mW/μm², or 1.7W/mm according to emitter length.

The device was found to operate stably at the large V_{CE} bias with no evidence of degradation. "Such device stability under aggressive large-signal operation suggests inherent reliability advantages in the InP–GaAsSb material system," the team comments.

The measurements were made without thermal management enhancements such as substrate thinning and/or transferring the devices to thermally conductive substrates, e.g. aluminium nitride or silicon carbide. ■

https://doi.org/10.1109/TED.2021.3138379

Author: Mike Cooke

REGISTER
for *Semiconductor Today*
free at
www.semiconductor-today.com